

High-temperature arc-parallel normal faulting and transtension at the roots of an obliquely convergent orogen

Keith A. Klepeis*

Department of Geology and Geophysics, Building F05, University of Sydney, New South Wales 2006, Australia

Maria Luisa Crawford*

Department of Geology, 101 North Merion Avenue, Bryn Mawr College, Bryn Mawr, Pennsylvania 19010, USA

ABSTRACT

Structural and kinematic data from northern coastal British Columbia (~54.5°N) document intra-arc deformation patterns at mid-crustal levels during and after emplacement of the Coast Mountains batholith. Major arc-parallel displacements occurred along high-temperature (700 °C) ductile normal faults and steep sinistral transtensional shear zones within an obliquely convergent margin. Strain patterns and pluton emplacement were controlled by (1) structural anisotropies in host rocks that predate batholith emplacement, and (2) kinematic compatibility requirements created by simultaneous motion on curved, pluton-bounding shear zones. These controls superseded a partitioning of the arc-parallel and arc-normal components of oblique-plate convergence onto strike-slip and thrust faults, respectively.

INTRODUCTION

Interpretations of intra-arc deformation and the kinematics of pluton emplacement are hindered by problems such as limited exposure of deep-crustal levels, complex three-dimensional variability in structure, and the inadequate memory of rock fabrics in deforming migmatites and granitoids (e.g., Paterson and Fowler, 1993; Grocott et al., 1994; Tobisch et al., 1995; Tikoff and de Saint Blanquat, 1997). In this paper we present evidence for a distinctive style of intra-arc ductile normal faulting and sinistral transtension at the roots of the latest Cretaceous to early Tertiary magmatic arc of the central Coast Mountains, British Columbia (Fig. 1). Excellent three-dimensional exposure of the deep roots of this system allowed us to examine (1) space-time relationships among arc-parallel, vertical, and arc-normal horizontal displacements within an obliquely convergent margin; (2) the kinematics and effects of deep-crustal deformation during and after batholith emplacement; and (3) the interplay between orogen-parallel deformation and pluton emplacement. We show that coeval pluton-bounding shear zones display widely different orientations and kinematics. The main controls on intraarc kinematic patterns were the reactivation of structural anisotropies and the geometry of linked shear-zone systems. Coordinated deformation in linked shear zones tectonically denuded and exhumed the deep roots of the batholith between 67 and 50 Ma.

MAJOR STRUCTURAL DOMAINS

The central Coast Mountains consist of three main structural domains: the western thrust belt, the Coast Mountains batholith, and the Coast shear zone (Fig. 1). The western thrust belt formed prior to 90 Ma and preserves a record of middle to lower crustal ductile thrust faulting and pluton emplacement (Monger et al., 1982; Crawford et al., 1987; Rubin and Saleeby, 1992). Little igneous activity occurred in the western thrust belt between ca. 90 Ma and the Miocene (Cook and Crawford, 1994). East of the thrust belt, a 75–100-km-wide belt of plutonic rocks, orthogneiss, and paragneiss compose the Coast Mountains batholith. Batholith emplacement occurred when relative motion between the Kula and North American plates was changing from near-orthogonal convergence to obliquely convergent, dextral strike-slip motion (Engebretson et al., 1985; Stock and Molnar, 1988). U-Pb dates (Crawford et al., 1997; G. Gehrels, 1998, personal commun.) indicate that the batholith was constructed from ca. 88 to 51 Ma and was deeply exhumed by 50 Ma (Hollister, 1982; Wood et al., 1991). The central

part of the batholith is composed of the Khyex sill complex (Fig. 2, inset), a 7–8-km-thick series of sheeted sills and orthogneisses that dip 30°–45° to the north and northeast. The western edge of the batholith contains the tabular Quottoon pluton (Fig. 2, inset).

The Coast shear zone (Fig. 1) forms a steep, orogen-parallel boundary between the western thrust belt and the Coast Mountains batholith. Two phases of arc-normal displacements occurred within this shear zone between ca. 65 and 55 Ma. The first phase (ca. 65–57 Ma) involved east-side-up reverse displacements (McClelland et al., 1992; Ingram and Hutton, 1994; Klepeis et al., 1998). The ca. 59–55 Ma Quottoon pluton (Gehrels et al., 1991) was emplaced into the shear zone during and after this phase. The second phase (ca. 57–55 Ma) of deformation involved east-side-down normal motion that juxtaposed the Coast Mountains batholith against the western thrust belt (Klepeis et al., 1998). The eastern boundary of the deeply exhumed part of the batholith is the ca. 60–50 Ma Shames mylonite zone, a greenschist facies, ductile normal fault that dips moderately (~30°) east and northeast (Heah, 1991).

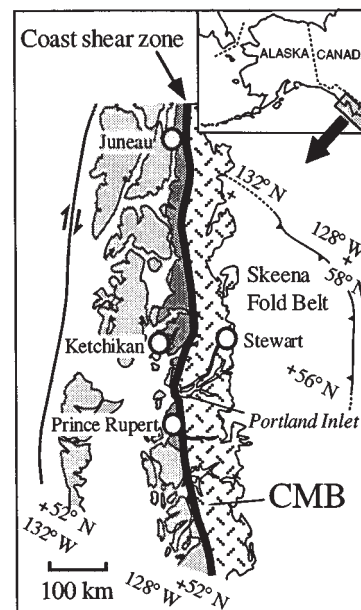


Figure 1. Tectonic map showing northern Coast Mountains batholith (CMB), Coast shear zone (bold line), and western thrust belt (dark, dotted pattern).

*E-mail: keith@es.su.oz.au; mcrawford@brynmawr.edu.

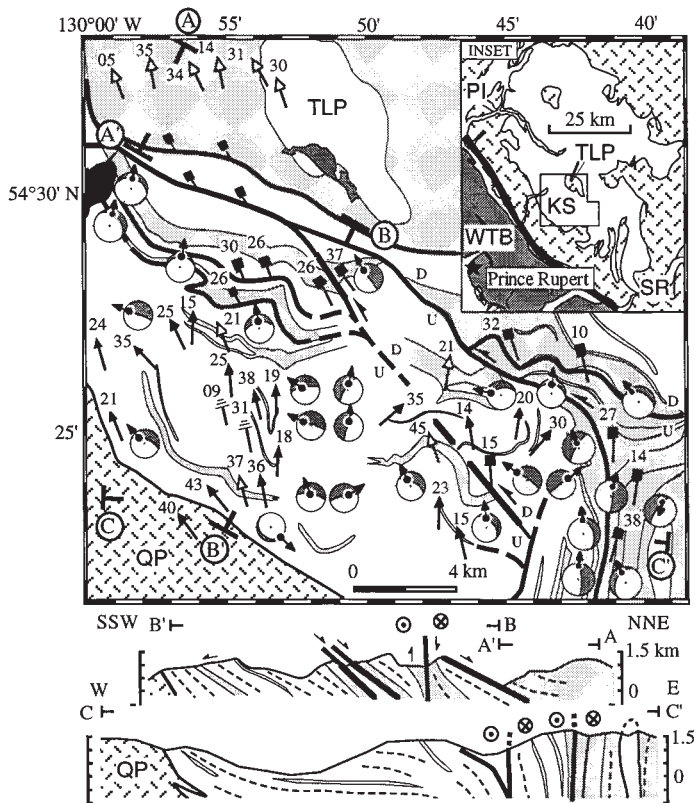


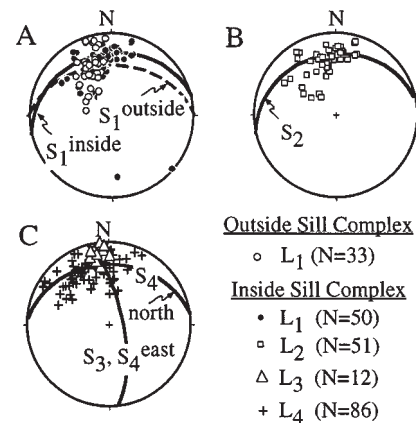
Figure 2. Structural and kinematic map of Khyex sill complex (KS in inset). North-northeast-south-southwest (A-A', B-B') and east-west (C-C') cross sections are shown. White represents type 2 sills; dotted pattern represents host-rock screens and type 1 sills, including Toon Lake pluton (TLP); random-dash pattern represents Quottoon pluton (QP). Black represents water-covered areas. Bold black lines are major ductile normal faults and sinistral transensional shear zones (D_4). Arrows show orientations of L_1 (white-ended arrows), L_2 (black-ended arrows), L_3 (arrows ending in three horizontal lines), and L_4 (black squares) lineations; numbers are plunge magnitudes. Equal-area plots show representative kinematics of 257 shear zones. Each plot shows orientation of shear zones (great circles), hanging wall (shaded), and direction of motion of hanging wall (arrows). All shear zones show normal or oblique-normal motion. In inset, PI is Portland Inlet, SR is Skeena River, bold line is trace of Coast shear zone, WTB is western thrust belt, random-dash pattern represents major plutons, and white areas are layered plutonic complexes, orthogneiss, and paragneiss.

STRUCTURAL RELATIONSHIPS

The oldest structures within the Coast Mountains batholith are preserved in metasedimentary and amphibolitic country rocks that host the Khyex sill complex and in one of two main types of tabular sills that compose the magmatic part of the sill complex. Host rocks located outside the sill complex and as conformable screens within it (Fig. 2) contain a moderately north-dipping, gneissic foliation (S_1) and moderately north- and northwest-plunging amphibole and biotite mineral lineations (L_1). Outside the sill complex, L_1 - S_1 forms the dominant regional fabric. Inside the sill complex, sills that contain L_1 - S_1 , defined here as type 1 sills, are homogeneous, fine-grained granodioritic orthogneisses. These orthogneisses are inter-layered with host rocks and are compositionally and texturally similar to Late Cretaceous granodiorite plutons located outside the sill complex (e.g., TLP in Fig. 2). Because they share the same L_1 - S_1 fabric, we grouped type 1 sills with host-rock screens in Figure 2.

The L_1 - S_1 within the sill complex is variably overprinted by a younger fabric (L_2 - S_2) that also occurs in type 2 sills. Type 2 sills do not contain L_1 - S_1 and are composed of a heterogeneous mix of coarse-grained tonalite,

Figure 3. Lower-hemisphere, equal-area plots of structural data. A: L_1 - S_1 inside and outside sill complex. B: L_2 - S_2 inside sill complex. C: S_4 from northern roof of sill complex (S_4 north), S_4 from eastern boundary of sill complex (S_4 east), L_3 - S_3 from central part of sill complex, and L_4 lineations.



minor gabbro, felsic and amphibolitic dikes, and migmatitic orthogneiss that form sheeted tabular packages. The internal structure of type 2 sills is dominated by a uniformly north-dipping (30° N), margin-parallel foliation (S_2) and north- and northwest-plunging feldspar, amphibole, and biotite mineral lineations (L_2). At the regional scale, L_2 - S_2 and the margins of type 2 sills parallel L_1 - S_1 , and the margins of type 1 sills (A and B in Fig. 3) but, at the mesoscale, local crosscutting relationships occur. In type 1 sills and host-rock screens, L_2 - S_2 is less penetrative than in type 2 sills and, in places, envelops lenses that are dominated by L_1 - S_1 . In these lenses and at the margins of type 2 sills, L_2 - S_2 truncates L_1 - S_1 . Inside type 2 sills, L_2 - S_2 displays both solid-state and magmatic textures. Outside type 2 sills, L_1 - S_1 and L_2 - S_2 display only solid-state textures. Solid-state textures are characterized by pressure shadows on feldspar porphyroclasts, broken grains, and evidence of dynamic recrystallization. Magmatic textures are characterized by coarse equant quartz, feldspar, and amphibole grains showing good to poor alignment, an absence of pressure shadows around porphyroclasts, and no evidence of dynamic recrystallization. L_2 - S_2 also invariably displays top-down-to-the-north kinematics, whereas L_1 - S_1 invariably displays top-up-to-the-south kinematics (kinematic data presented in the following).

In some central areas of the sill complex, L_1 - S_1 and L_2 - S_2 are folded by upright folds (F_3) that display steeply west- and east-dipping axial planes and gently north-plunging axes. A solid-state foliation (S_3), defined by aligned biotite grains and flattened quartz-feldspar aggregates, parallels fold axial planes. Gently north-plunging biotite and amphibole mineral lineations (L_3) occur on S_3 surfaces and parallel F_3 axes and the L_1 and L_2 lineations (Fig. 3).

Within the upper part and at the roof of the sill complex, a series of subparallel, north-dipping ($\sim 30^\circ$ N) shear zones (D_4) crosscut L_1 - S_1 , L_2 - S_2 , and L_3 - S_3 - F_3 structures. These shear zones contain north- and northwest-plunging sillimanite and amphibole mineral lineations (L_4) and a solid-state foliation (S_4) that strikes east-west and dips northward (C in Fig. 3). At the regional scale, S_4 parallels S_1 and S_2 . At the mesoscale and in high-strain areas, L_1 - S_1 , L_2 - S_2 , and L_3 - S_3 - F_3 are transposed parallel to S_4 . In lower-strain areas, L_1 - S_1 and L_2 - S_2 occur as slightly more northeast-striking fabrics that are truncated by S_4 . In this area, leucotonalite dikes crosscut L_2 - S_2 and L_3 - S_3 - F_3 and contain L_4 - S_4 .

At the northeastern and eastern sides of the sill complex, the D_4 shear zones that formed at the sill roof change orientation and merge into a major subvertical, north-striking, 4-km-wide shear zone (Fig. 2). This north-striking shear zone forms the eastern boundary of the sill complex and contains north- and northwest-plunging sillimanite and amphibole mineral lineations (L_4) that parallel L_4 lineations at the sill roof (C in Fig. 3). At the mesoscale, a vertical, north-striking foliation (S_4) within this shear zone truncates L_1 - S_1 and L_2 - S_2 at near-orthogonal angles. L_3 - S_3 - F_3 structures do not occur in this area. At the regional scale, L_1 - S_1 and L_2 - S_2 are reoriented parallel to the subvertical orientation of S_4 (cross section C-C' in Fig. 2).

Northwest of the sill roof, another major shear zone that gradually merges with the gently north-dipping shear zones at the sill roof strikes northwest and dips moderately northeast. Inside the sill complex, hundreds of shear zones displaying trace lengths from a few meters to several kilometers long crosscut L_1-S_1 , L_2-S_2 , and $L_3-S_3-F_3$ structures. A steep to subvertical, northwest-striking set is dominant in terms of size (trace lengths of hundreds of meters to 2 km) and abundance (>67% of 257 measured). A northeast-striking set displays dips ranging from gentle to steep to the southeast and northwest. Posttectonic aplite dikes and pegmatites crosscut all L_1-S_1 , L_2-S_2 , L_3-S_3 , and L_4-S_4 fabrics.

KINEMATIC RELATIONSHIPS

All kinematic indicators discussed here were viewed on surfaces parallel to mineral lineations and perpendicular to foliations. For each phase of deformation, boudinage confirmed that these are true stretching directions. Kinematic indicators within the L_1-S_1 fabric both inside and outside the sill complex include C' shear bands, oblique foliations, and asymmetric tails on feldspar porphyroclasts (a and d in Fig. 4) that show top-up-to-the-south, thrust-type displacements. Where the L_2-S_2 fabric displays solid-state textures in type 1 and 2 sills, C' shear bands, S-C fabrics, and asymmetric tails on feldspar porphyroclasts record top-down-to-the-north and -northwest normal displacements (c and f in Fig. 4). Where L_2-S_2 is magmatic in type 2 sills, melt-filled shear bands also record normal displacements. Kinematic indicators within L_3-S_3 include C' shear bands that record subhorizontal sinistral displacements (e in Fig. 4).

Within D_4 shear zones located at and near the roof of the sill complex, asymmetric boudinage, S-C fabrics (b in Fig. 3), C' shear bands, and

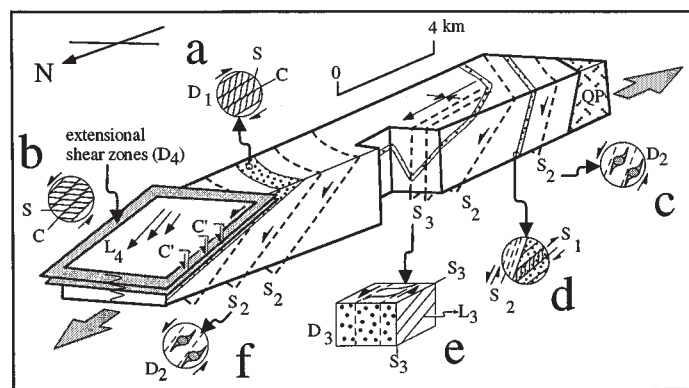


Figure 4. Three-dimensional block diagram showing spatial relationships between structures within Khyex sill complex. Patterned horizons are host rocks. Individual sketches are as follows: (a) D_1 kinematics in host-rock screen, (b) D_4 kinematics at sill roof, (c) D_2 kinematics in type 1 and type 2 sills, (d) D_2 - D_1 overprinting relationships at margins of type 2 sill and host rocks, (e) D_3 kinematics, (f) D_2 kinematics in type 2 sills. QP—Quottoon pluton.

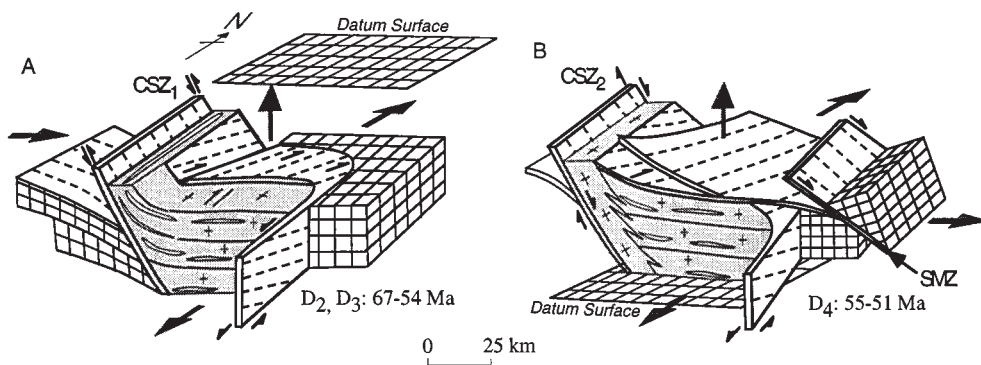


Figure 5. Two-phase model of deformation accompanying emplacement and denudation of Coast Mountains batholith. Bold surfaces are major pluton-bounding shear zones; dashed lines show displacement directions; shaded areas are plutons. A: D_2 and D_3 during and after type 2 sill emplacement; CSZ1 is first phase (reverse) of Coast shear zone deformation. B: Final stage (D_4) of transtensional denudation of orogen; CSZ2 is second phase (normal) of Coast shear zone deformation, and SMZ is Shames mylonite zone.

oblique foliations in asymmetric low-strain pods indicate top-down-to-the-north and -northwest normal displacements. In the steep shear zones at the eastern boundary of the sill complex, sinistral displacements are indicated by C' shear bands, asymmetric boudinage, and asymmetric recrystallized tails on feldspar and garnet porphyroblasts. Normal and oblique-normal displacements in the D_4 shear zones distributed inside the sill complex are summarized by equal-area plots in Figure 2.

ABSOLUTE TIMING OF DEFORMATION

U-Pb isotopic analyses on single zircons from within and outside the sill complex yielded the following dates (Crawford et al., 1997; G. Gehrels, 1998, personal commun.): Type 1 sills range from ca. 88 to 71 Ma; the main tonalite bodies of type 2 sills yielded ca. 67–64 Ma ages. Because L_1-S_1 occurs in type 1 sills but does not occur within type 2 sills, D_1 deformation occurred during or after the interval 88–71 Ma and before 67 Ma. The ages of type 2 sills and magmatic L_2-S_2 textures indicate that D_2 ductile normal faulting coincided with ca. 67–64 Ma type 2 sill emplacement. A 54 Ma leucotonalite sill that crosscuts L_2-S_2 but contains L_4-S_4 indicates that D_2 ended by 54 Ma. Crosscutting relationships between L_4-S_4 and $L_3-S_3-F_3$ and a 64 Ma type 2 sill that contains F_3 folds of L_2-S_2 indicate that D_3 initiated after 64 Ma and also ended by 54 Ma. Hence, D_2 and D_3 coincided with arc-normal displacements in the Coast shear zone. D_4 at the boundaries of the sill complex outlasted D_2 , D_3 , and emplacement of the ca. 59–55 Ma Quottoon pluton, and could have initiated anytime after 64 Ma. Posttectonic pegmatites that crosscut D_2 , D_3 , and D_4 fabrics all yielded ca. 51–50 Ma ages.

INTERPRETATION OF DEFORMATION PATTERNS

Our structural and kinematic analyses suggest that the north-dipping D_4 shear zones near and at the roof of the Khyex sill complex and the steep, sinistral D_4 shear zones on the eastern side of the sill complex formed a kinematically linked system. Geochronologic data and consistent crosscutting relationships indicate that arc-parallel displacements in these shear zones occurred simultaneously or episodically between 54 and 51 Ma and possibly earlier. The shear zones form an interconnected network of surfaces that merge and change orientation at the boundaries of the sill complex (Fig. 2). Where the shear zones are steep, they accommodated sinistral strike-slip motion, and where the shear zones dip moderately northward, they formed ductile normal faults. Despite this variability, L_4 lineations within all segments of the shear zones are approximately parallel (C in Fig. 3). This approximate parallelism indicates that top-down-to-the-north and -northwest normal displacements at the roof were kinematically compatible with sinistral motion at the sides of the sill complex (A in Fig. 5). Simultaneous or episodic, arc-parallel sinistral transtensional displacements in curved, interconnected shear zones explains the three-dimensional complexity of D_4 kinematics.

A coordinated sinistral transtensional displacement field like the one we have suggested for D_4 also explains geometric, kinematic, and space-time relationships between D_2 , D_3 , and the emplacement of type 2 sills. First, the approximate parallelism of L_2 , L_3 , and L_4 (Fig. 3) and identical

kinematic patterns on surfaces of similar orientation suggest that D_2 , D_3 , and D_4 reflect similar displacement fields. For example, the sense and direction of normal displacement on north-dipping S_2 surfaces during D_2 was identical to that on north-dipping S_4 surfaces during D_4 . Similarly, the sense and direction of sinistral displacement on subvertical, north-striking S_3 surfaces during D_3 was identical to that on the north-striking, subvertical S_4 surfaces. Second, geochronologic data indicate that 67–54 Ma D_2 normal displacements occurred either diachronously with or shortly before 64–54 Ma sinistral displacements during D_3 . These data also support the interpretation that D_2 and D_3 structures formed during simultaneous or episodic sinistral and normal displacements. Finally, we suggest that arc-parallel ductile normal faulting coupled with arc-parallel sinistral motion transferred host rocks parallel to the orogen to accommodate the emplacement of type 2 sills (A in Fig. 5). This interpretation is supported by the following observations: (1) the onset of 67–64 Ma D_2 normal faulting occurred simultaneously with the emplacement of the first type 2 sills; (2) all type 2 sills are located in the footwall of north-dipping D_4 normal faults at the roof of the sill complex and are bounded elsewhere by sinistral shear zones; and (3) type 2 sills are tabular, sheeted, and parallel S_2 and S_4 surfaces.

The regional parallelism of L_1 - S_1 and L_2 - S_2 (cf. A and B in Fig. 3) suggests that S_1 surfaces controlled the geometry of the L_2 - S_2 fabric during D_2 arc-parallel stretching. In areas unaffected by younger folding and the D_4 shear zones, the nearly identical orientations of L_1 - S_1 inside and outside the sill complex (A in Fig. 3) indicate that D_2 deformation did not significantly alter the orientation of L_1 - S_1 at the regional scale. Both D_2 and type 2 sills conform to the geometry of the preexisting L_1 - S_1 fabric. The parallelism of S_1 , S_2 , and S_4 in the roof zone of the sill complex indicates that S_1 orientations continued to influence the structure of the sill complex during D_4 . A direct result of this reactivation of S_1 surfaces by ductile normal faults during D_2 and D_4 was the denudation and eventual exhumation of the deep roots of the central Coast Mountains batholith prior to 50 Ma.

Arc-parallel and oblique displacements within and at the boundaries of the Khyex sill complex contrast with coeval arc-normal displacements in the adjacent Coast shear zone. We suggest that the partitioning of arc-normal displacements in the Coast shear zone occurred because this shear zone was not physically or kinematically linked to intra-arc normal faults or curved sinistral shear zones. Whereas normal and sinistral shear zones accommodated arc-parallel displacements inside the batholith, ca. 65–57 Ma east-side-up displacement in the Coast shear zone appears to reflect one or a combination of the following: (1) inflation of its hanging wall (eastern side) with magma (the type 2 sills and the Quottoon pluton), (2) vertical displacement of the central Coast Mountains batholith as a result of its unroofing by normal faulting (A in Fig. 5), or (3) contraction across the arc. East-side-down, arc-normal displacements in the Coast shear zone ca. 57–55 Ma and ca. 60–50 Ma top-down-to-the-east displacements in the Shames mylonite zone reflect a period when normal faulting dominated the central Coast Mountains batholith during the final stages of its denudation and exhumation (B in Fig. 5). These styles of deformation in the central Coast Mountains imply that factors such as kinematic compatibility and the reactivation of preexisting anisotropies superseded a partitioning of the arc-parallel and arc-normal components of oblique plate convergence into strike-slip and thrust faults, respectively.

CONCLUSIONS

Highly variable kinematic patterns and pluton emplacement at deep levels within the central Coast Mountains batholith were controlled by a reactivation of preexisting structural anisotropies and the effects of simultaneous, kinematically compatible displacements within curved shear zones. Arc-parallel displacements were accommodated by ductile normal faults and coeval sinistral transtensional shear zones. These shear zones controlled the location and geometry of pluton emplacement and tectonically denuded the deep roots of the central Coast Mountains batholith between ca. 67 and 50 Ma.

ACKNOWLEDGMENTS

Work for this paper was funded by the National Science Foundation (NSF) Continental Dynamics Program as part of the ACCRETE project. Additional funding was provided by an NSF Postdoctoral Fellowship to Klepeis and NSF grant EAR-9304321 to Crawford. We thank L. Hollister, C. Davidson, C. Andronicos, D. Chardon, K. Sinha, G. Gehrels, and G. Mora for helpful discussions and G. Axen, L. P. Gromet, and J. Oldow for helpful reviews.

REFERENCES CITED

- Cook, R. D., and Crawford, M. L., 1994, Exhumation and tilting of the western metamorphic belt of the Coast orogen in southern southeastern Alaska: *Tectonics*, v. 13, p. 528–531.
- Crawford, M. L., Hollister, L. S., and Woodsworth, G. J., 1987, Crustal deformation and regional metamorphism across a terrane boundary, Coast plutonic complex, British Columbia: *Tectonics*, v. 6, p. 343–361.
- Crawford, M. L., Gehrels, G. E., Klepeis, K. A., and Crawford, W. A., 1997, Latest Cretaceous and Paleogene history of the central region of the Coast orogen at the British Columbia–Alaska border: *Geological Society of America Abstracts with Programs*, v. 29, no. 6, p. 83.
- Engelbreton, D. C., Cox, A., and Gordon, R. G., 1985, Relative motions between oceanic and continental plates in the Pacific Basin: *Geological Society of America Special Paper* 206, 59 p.
- Gehrels, G. E., McClelland, W. C., Samson, S. D., Patchett, P. J., and Brew, D. A., 1991, U–Pb geochronology of Late Cretaceous and early Tertiary plutons in the northern Coast Mountains batholith: *Canadian Journal of Earth Sciences*, v. 28, p. 899–911.
- Grocott, J., Brown, M., Dallmeyer, R. D., Taylor, G. K., and Treloar, P. J., 1994, Mechanism of continental growth in extensional arcs: An example from the Andean plate boundary zone: *Geology*, v. 22, p. 391–394.
- Heah, T. S. T., 1991, Mesozoic ductile shear and Paleogene extension along the eastern margin of the Central Gneiss complex, Coast belt, Shames River area, near Terrace, British Columbia [M.S. thesis]: Vancouver, University of British Columbia, 155 p.
- Hollister, L. S., 1982, Metamorphic evidence for rapid (2 mm/yr) uplift of a portion of the Central Gneiss complex, Coast Mountains, British Columbia: *Canadian Mineralogist*, v. 20, p. 319–332.
- Ingram, G. M., and Hutton, D. H. W., 1994, The Great Tonalite sill: emplacement into a contractional shear zone and implications for Late Cretaceous to early Eocene tectonics in southeastern Alaska and British Columbia: *Geological Society of America Bulletin*, v. 106, p. 715–728.
- Klepeis, K. A., Crawford, M. L., and Gehrels, G. A., 1998, Structural history of the crustal-scale Coast shear zone near Portland Inlet, SE Alaska and British Columbia: *Journal of Structural Geology*, v. 20, p. 883–904.
- McClelland, W. C., Gehrels, G. E., Samson, S. D., and Patchett, P. J., 1992, Structural and geochronologic relations along the western flank of the Coast Mountains batholith: Stikine River to Cape Fanshaw, central SE Alaska: *Journal of Structural Geology*, v. 14, p. 475–489.
- Monger, J. W. H., Price, R. A., and Templeman-Kluit, D. J., 1982, Tectonic accretion and the origin of the two major metamorphic and plutonic belts in the Canadian Cordillera: *Geology*, v. 10, p. 70–75.
- Paterson, S. R., and Fowler, T. K., 1993, Extensional pluton-emplacement models: Do they work for large plutonic complexes?: *Geology*, v. 21, p. 781–784.
- Rubin, C. M., and Saleeby, J. B., 1992, Tectonic history of the eastern edge of the Alexander terrane, southeast Alaska: *Tectonics*, v. 11, p. 586–602.
- Stock, J., and Molnar, P., 1988, Uncertainties and implications of the Late Cretaceous and Tertiary position of North America relative to the Farallon, Kula and Pacific plates: *Tectonics*, v. 7, p. 1339–1384.
- Tikoff, B., and de Saint Blanquat, M., 1997, Transpressional shearing and strike-slip partitioning in the Late Cretaceous Sierra Nevada magmatic arc, California: *Tectonics*, v. 16, p. 442–459.
- Tobisch, O. T., Saleeby, J. B., Renne, P. R., McNulty, B., and Weixing, T., 1995, Variations in deformation fields during development of a large-volume magmatic arc, central Sierra Nevada, California: *Geological Society of America Bulletin*, v. 107, p. 148–166.
- Wood, D. J., Stowell, H. H., Onstott, T. C., and Hollister, L. S., 1991, $^{40}\text{Ar}/^{39}\text{Ar}$ constraints on the emplacement, uplift, and cooling of the Coast Plutonic Complex sill, southeastern Alaska: *Geological Society of America Bulletin*, v. 103, p. 849–860.

Manuscript received June 3, 1998

Revised manuscript received September 28, 1998

Manuscript accepted October 14, 1998